



HAL
open science

Impact of green walls occultation on energy balance: Development of a TRNSYS model on a brick masonry house

Mohamed-Amine Kenai, Laurent Libessart, Stéphane Lassue, Didier Defer

► To cite this version:

Mohamed-Amine Kenai, Laurent Libessart, Stéphane Lassue, Didier Defer. Impact of green walls occultation on energy balance: Development of a TRNSYS model on a brick masonry house. *Journal of Building Engineering*, 2021, 44, pp.102634. 10.1016/j.job.2021.102634 . hal-03230581

HAL Id: hal-03230581

<https://hal.science/hal-03230581v1>

Submitted on 16 Jun 2022

HAL is a multi-disciplinary open access archive for the deposit and dissemination of scientific research documents, whether they are published or not. The documents may come from teaching and research institutions in France or abroad, or from public or private research centers.

L'archive ouverte pluridisciplinaire **HAL**, est destinée au dépôt et à la diffusion de documents scientifiques de niveau recherche, publiés ou non, émanant des établissements d'enseignement et de recherche français ou étrangers, des laboratoires publics ou privés.

1 Impact of green walls occultation on energy balance:

2 Development of a TRNSYS model on a brick masonry house

3 Mohamed-Amine Kenai¹, Laurent Libessart², Stéphane Lassue², Didier Defer²

4 ¹ JUNIA-HEI, ULR 4515, Laboratoire de Génie Civil et géo-Environnement (LGCgE), F-59000 Lille,
5 France

6 ² Univ.Artois, ULR 4515, Laboratoire de Génie Civil et géo-Environnement (LGCgE), F-62400
7 Béthune, France

8 *Corresponding author: Laurent Libessart, laurent.libessart@univ-artois.fr

9

10 **Abstract**

11 This study is interested in the evaluation of the development of extensive green walls (GWs)
12 on the energy balance of buildings with a global code of dynamic thermal simulation of
13 buildings under TRNSYS. In fact, green walls are not integrated into the thermal simulation
14 during thermal calculations. For, the "Type" developed was used to make a new contribution to
15 the prediction of the thermal behavior of green walls. The first part presents the equations
16 integrated in the model. A description of the dynamic thermal simulation software is carried
17 out as well as the methods of integration of the developed model. Then, the modeling of the
18 influence of GW (Ivy or Virginia Creeper) on a more global scale is detailed. It highlights the
19 thermal and energy impact of GWs in winter and summer on a brick house located in Lille in
20 France. This is a concrete case of representation of an existing residential building in an urban
21 environment to help thermal design offices to take them into account in the simulations. It has
22 been shown that the presence of vegetation protects the facades against summer overheating
23 and therefore reduces the energy requirements for air conditioning. In winter, the use of
24 deciduous plants on facades exposed to the sun makes it possible to benefit from solar radiation

25 and limit the demand for energy for heating. Finally, the GWs technique is more suitable for
26 the thermal renovation of weakly insulated buildings.

27 Keywords: extensive green walls, dynamic simulation, building, TRNSYS, thermal behavior

28

29

30 Nomenclature

Symbols :

T temperature, K

GW Green wall

GWs Green walls

I_s^\downarrow incident solar radiation, W/m²

F leaf cover index

W_{CC} Cellular Concrete Wall

Greek letters :

α solar absorption coefficient

β_{zen} solar zenith angle

φ flux density, W/m²

σ constant of Stefan-Boltzmann

σ_{occ} coverage rate, [0,1]

ε emissivity, [0,1]

τ transmissivity, [0,1]

σ_{GW} coverage rate, [0,1]

μ^* solar extinction coefficient

Indices / Exponents :

CC cellular concrete

Eq equivalent

sol solar

R_{env} infrared exchanges with the
environment

R_{occ} infrared exchanges with the GW

R_{env} infrared exchanges with the
environment

R_{occ} infrared exchanges with the GW

R_{env-CC} infrared exchanges with the
environment

R_{GW-CC} infrared exchanges with the GW

cv convection

31 **I. Introduction**

32 The use of green walls came mainly from Germany in the early 1970s. The aesthetic aspect and
33 the desire to bring originality to buildings was often the main reason for creating a green wall
34 [1]. Its usefulness was subsequently oriented to mainly counter the phenomenon of urban heat
35 island which results in a temperature difference between a rural and urban area in the same
36 region [2-4]. Most of the experiments in in-situ conditions on the thermal benefits of green
37 walls make comparisons between buildings with or without green walls [5-11]. The results
38 cannot be generalized, unless all the parameters that can influence the building's energy balance
39 have been considered or measured, which is very complicated to achieve. It is also recognized
40 that interior temperatures are strongly influenced by the occupants and their behavior (cooling
41 and heating system, opening / closing of doors and windows, manipulation of window curtains,
42 etc.) and it is very difficult to obtain precise technical information throughout the year unless
43 the building is pre-equipped with a set of sensors capable of collecting the necessary data [12-
44 16]. In addition, it is not possible to ask for the same scenarios or modes of use for all the
45 occupants of the different buildings studied and this can therefore generate significant
46 differences and affect the comparisons.

47 Green walls can also have very positive effects on improving sound insulation [17-19]. Green
48 walls are used more and more as a means of fighting against urban climate warming, especially
49 in the case of tropical climates [20-22] or to reduce consumption of heating or air conditioning
50 [23]. Moreover, many studies, green walls contribute to the improvement of air quality [24,25]
51 and bring biodiversity to urban centers [3]. The integration of green walls in dynamic thermal
52 simulation codes is little used for the calculation of the energy balance [26-28] or for special
53 cases, such as the study of solar greenhouses [29]. Numerical simulation has been used more to
54 study green roofs to reduce heat islands and overheating in summer [30-35] or to improve the
55 energy efficiency of an entire building [36,37]. Experimental research done on radiative

56 occultation by extensive green walls (ivy and Virginia creeper) has shown good conclusions
57 [8]. Three boxes had been instrumented to collect all the information necessary for the creation
58 of the numerical model. In addition, this model for the prediction of the thermal influence of
59 extensive green walls was validated at the scale of the experimental model [38]. The results are
60 very encouraging. To finalize the study, the quantitative analysis must be extrapolated to a real
61 scale of a building. Various software can be used for the dynamic simulation of greenhouses
62 [39]. In our case, the coupling of the green wall model focused on the use of the global dynamic
63 thermal building simulation code TRNSYS. This software was used in our laboratory for the
64 study of solar walls [40, 41]. TRNSYS is often used for estimating energy consumption in
65 buildings [42,43]. Modeling the influence of GWs on a more global scale will highlight, through
66 several scenarios, the thermal influence of GWs on the thermal balance of an old brick house
67 located in Lille (France). A first study on the thermal conductivity of the materials composing
68 green walls (intensive and extensive) had shown that green walls could be used as an additional
69 insulation [44]. It is therefore an application to a representative study of an existing residential
70 building in an urban environment in the north of France in a degraded oceanic climate. That is,
71 these regions have more mixed characteristics, with less rain in winter, and more thunderstorms
72 in summer. These climates average roughly the same amount of rain each month of the year.
73 The temperature contrasts are also more important there [45]. The aim of this study is to show
74 the advantages and disadvantages of green walls in winter and summer. This tool would also
75 allow construction companies to better use this technique in the construction and integration of
76 the energy balance. The first part is introduced by the description of the simulation software
77 used, and the integration of the model developed in this same software. The second part will
78 focus on modeling the influence of GWs on a more global scale and quantifying the heating or
79 air conditioning needs.

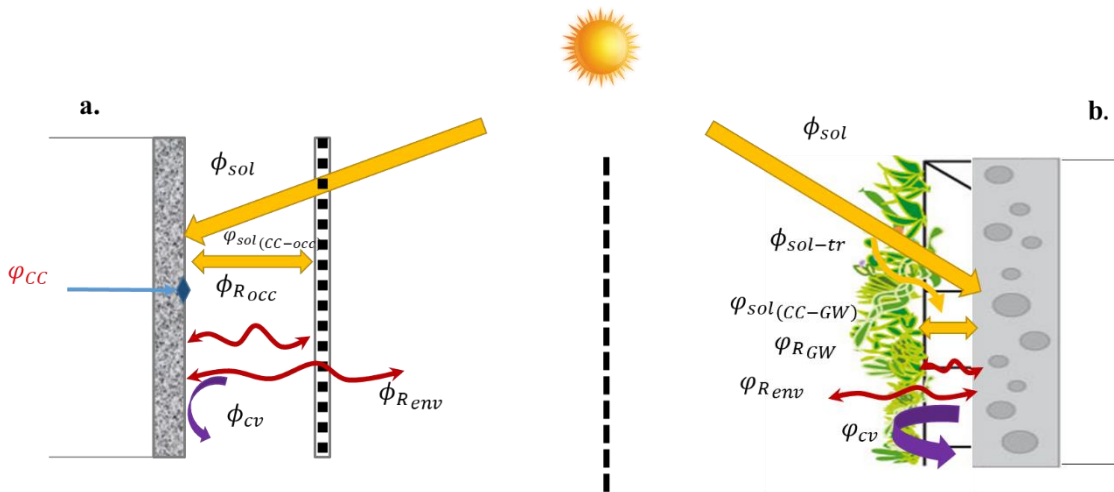
80 II. Materials and Method

81 2.1. Equations to the case of vegetation

82 As explained in a previous publication [38], the digital model has been described and validated.
 83 To provide a better understanding of the simulations that will be developed in this research, the
 84 modifications of the equations with the presence of a green wall (GW) are recalled. The energy
 85 balance at a wall obscured by vegetation is based on the balance equations of solar radiation
 86 exchanges, infrared exchanges, and convective exchanges (Equation 1).

$$87 \quad \varphi_{cc} = \varphi_{sol} - \varphi_{R_{env-CC}} - \varphi_{R_{GW-CC}} - \varphi_{cv} \quad (1)$$

88 Figure 1 shows the differences in parameters between an artificial occultation and a vegetated
 89 occultation.



90 **Fig. 1: Elements of the energy balance ;(a) case of artificial obscuration ; (b) case of**
 91 **masking by the vegetation [30]**

92 As explained [38], the second important difference is related to the geometry of the occultation.
 93 The thickness of the leaf layer, the density and the number of leaves are new parameters to be
 94 integrated into the energy balance equations. This last aspect requires modification of the
 95 transmitted and absorbed solar radiation and an adaptation of the equations of convective
 96 exchanges. These convective exchanges are considered in the case of the artificial occultation

97 to be similar to exchanges between two flat surfaces. They are more complex in the case of
 98 plants, and it is then necessary to consider an aerodynamic resistance in the external surface
 99 area of the leaf layer and a resistance to the sensible heat transfer within the canopy layer,
 100 following its thickness, and the density of leaves.

101 The radiative exchanges balance was also adapted according to the characteristics of the plants,
 102 no change was made to the infrared radiation equations on one hand and between the GW and
 103 the cellular concrete wall (W_{CC}) on the other hand (Equation 2):

$$104 \quad \varphi_{R_{GW-CC}} = \frac{\sigma \times (T_{CC}^4 - T_{GW}^4)}{\frac{1 - \varepsilon_{CC}}{\varepsilon_{CC}} + \frac{1}{\sigma_{GW}} + \frac{1 - \varepsilon_{GW}}{\varepsilon_{GW}} \times \frac{1}{\sigma_{GW}}} \quad (2)$$

105 Since the leaf layer of plants is considered semi-transparent to solar radiation, a transmitted flux
 106 term has been added (φ_{sol-tr}). This adds to the direct solar flux and to those exchanged
 107 between the masking and the WCC have been expressed respectively by ($\varphi_{sol(GW-CC)}$) in
 108 equations (3).

$$109 \quad \varphi_{sol(GW-CC)} = I_s^\downarrow \times \alpha_{CC} (1 - \sigma_{GW}) \times \sum_{n=2}^{\infty} r_{CC}^n (\sigma_{GW} \times r_{GW})^{n-1} \quad (3)$$

110 The radiative flux transmitted by the foliar layer of plants (φ_{sol-tr}), is obtained as a function
 111 of the incident solar radiation, the WCC absorption coefficient, the coverage rate of the plant
 112 layer and the solar transmission coefficient of the leaf layer (Equation 4).

$$113 \quad \varphi_{sol-tr} = I_s^\downarrow \times \alpha_{CC} \times \sigma_{CC} \times \tau_{GW} \quad (4)$$

114 Thus, the coefficient (τ_{GW}) is calculated as a function of the solar zenith angle (β_{zen}), the leaf
 115 coverage index (F) and a solar extinction coefficient (μ^*) which vary according to the radiative
 116 properties of the leaves and their mean inclination (Equation 5).

$$117 \quad \tau_{GW} = \exp(-\mu^* \times \beta_{zen} \times F) \quad (5)$$

118 The inclination of the leaves and the radiative properties of the plants (μ^*) determine the depth
 119 up to which direct solar radiation (of β zenith angle) can penetrate in the leaf layer without

120 being intercepted. The foliar cover index (F), for its part, is a dimensionless quantity,
121 representing the spatial distribution of the leaf structure in three dimensions. In other words,
122 the index F is taken to be equal to the coverage rate in the case of a spatial distribution in 2D
123 only (case of artificial occultation). It is defined as the ratio between half of the total surface
124 area of the leaves (up and down seeds) and the total surface area (W_{cc}). Unlike the coverage
125 rate, which is limited to the ratio between the covered area and the total area, the index F is
126 calculated taking into account the total number of leaves, even if they are superimposed
127 (Equation 6).

$$F = \frac{1/2 \text{ Total leaf area}}{W_{cc} \text{ area}} \quad (6)$$

130 The numerical model equations have been validated allow a modeling of the thermal effect of
131 vegetation on buildings on a real scale [38]. This developed digital tool provides more precision
132 on the effects of vegetation in regions with a temperate climate. It can now be integrated into
133 thermal building simulation software (TRNSYS). It will also make it possible to study the
134 thermal effects of simple green walls in other climates and for different types of constructions.

135 2.2. *Building modeling using TRNSYS*

136 The theoretical study developed in this research focused on the thermal exchanges between
137 building facades and the external environment in the presence of green walls. For the model to
138 be validated, it was necessary to introduce a junction temperature (or heat flow) to the modeled
139 surface (instrumented wall). On the real scale of the building, it will be necessary to consider
140 all the thermal phenomena influencing this junction temperature, hence the interest of coupling
141 the model developed with a global code for dynamic thermal simulation of buildings. The
142 model developed predicts the thermal behavior of green walls.

143 By integrating it into the overall code, it will be possible to assess the influence of the presence
144 of green walls on the building's energy balance.

145 The choice of simulation software was the "TRNSYS" simulation environment [26, 46], which
146 stands for "Transient System Simulation Program" (TRaNsient SYstem Simulation program).

147 The strong point of TRNSYS is its modularity. Indeed, simulations under TRNSYS are based
148 on links between several dynamic systems created through the graphical interface (TRNStudio).

149 Each system is represented by an open component (TYPE) containing a pre-implemented code
150 for modeling it. This flexibility allows TRNSYS to integrate all the characteristics of the
151 building (geometry, construction materials, overall architecture ...), equipment (heating or air
152 conditioning system, ventilation, ...) and user behavior. The simulation of buildings under
153 TRNSYS is carried out with a multi-zone building code. This is the "Type 56" which uses an
154 external "TRNBuild" program during simulations.

155 The "TRNBuild" allows the user to define the geometry of the building (the geometry can also
156 be imported from a 3D drawing), the number of thermal zones to be modeled, and the different
157 characteristics of the materials. It is used to manage occupancy scenarios, define the air
158 infiltration rate, and control the set point temperatures for the heating and air conditioning
159 systems. Using the "TRNBuild" software environment the walls should be defined as either
160 external walls (with orientation specification) or internal walls adjacent to a defined thermal
161 zone. The program can take into account several layers of materials for each type of wall
162 (multilayer walls), the characteristics of most conventional materials being listed in a database
163 accessible from TRNBuild. External thermal stresses are applied through a link with a weather
164 file (Type 99: data defined by the user or Type 15: typical files and historical data by city)
165 according to the geographical position of the building and the orientation of each of the walls
166 exterior. Solar masks can be interposed between the outputs of the weather file and the "Type
167 56" inputs by adding a "Type 67" component dedicated to the projection of incident solar

168 radiation on the building envelope in the presence of a distant solar mask (immediate
169 environment of the construction). In addition, local thermal excitations can also be applied to a
170 wall, if the boundary conditions thereof are known.

171 When the "Type 56" is configured via the "TRNBuild" interface and linked with the
172 meteorological data on the "TRNStudio", it allows annual simulations to be carried out for
173 different thermal zones (room, floor, etc.) or for the whole building. Thus, the user will be able
174 to analyze the variations in the temperatures of the exterior and interior surfaces of each wall,
175 and the variations of the air temperatures at the level of each thermal zone. It will also be able
176 to assess the heating and / or air conditioning energy needs and establish detailed energy
177 balances for the building as a whole or only part of it. The calculations made with the "Type
178 56" are based on establishing the energy balance equations in each of the thermal zones.
179 Regarding the convective heat flow, the equations used by the "Type 56" consider the sum of
180 the following terms to perform an aeraulic heat balance:

- 181 - Convective exchanges with the interior surfaces of the walls ($Q_{\text{surf}, i}$),
- 182 - The contributions of infiltration of outside air ($Q_{\text{inf}, i}$),
- 183 - The contributions of ventilation,
- 184 - Thermal gains from internal convective exchanges "occupants, equipment, lighting,
185 heaters, etc.",
- 186 - Convective exchanges with the adjacent zone.

187 In addition, the convective heat flow in a thermal zone considers the fraction of solar gains
188 transmitted by any glazing, which immediately transforms into significant internal convective
189 gains. The solar flux absorbed by interior solar masking devices "interior curtains" which
190 directly transforms into sensible convective gains in the interior air is also considered.

191 Regarding the radiative energy balance inside a thermal zone, the equation under TRNSYS
192 considers the:

- 193 - Internal radiative contributions,
- 194 - Radiative flux transmitted by the glazing,
- 195 - Infrared exchanges with the internal surfaces of the area,
- 196 - Possible radiative thermal gains defined by the user.

197 Each thermal zone is then considered as an air node whose temperature is approximated either
198 by the standard method (by default on TRNSYS) by combining the radiative and convective
199 flows according to a star network [47], or by using a model of detailed transfer [48, 49], with
200 which radiative and convective fluxes are treated separately.

201 The standard model, unlike the detailed one, uses a fictitious temperature called (Tstar) which
202 combines the convective and radiative exchanges between the walls of the zone. While the
203 detailed one, treats convective and radiative exchanges separately. In terms of results, the
204 energy balances evaluated with the standard model are very similar to those evaluated by the
205 detailed calculation method [50]. The similarity is all the more confirmed in the case of multi-
206 zone buildings. For a study case with a single thermal zone, the detailed method is preferred
207 [51]. With regard to heat transfer by conduction, the heat flux at the walls is modeled in
208 TRNBuild by the method of weighting factors in the form of time series of surface temperatures
209 and heat fluxes [52, 53].

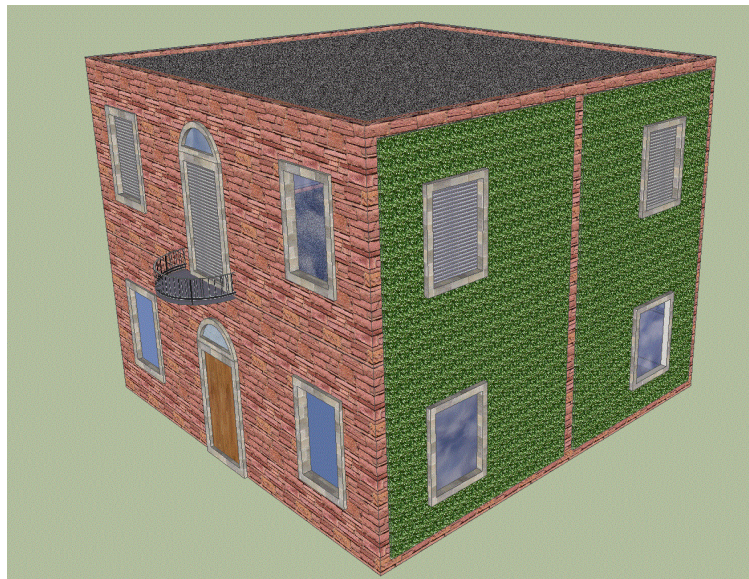
210 The digital study of the thermal interest of green walls [38] has shown the impact of occultation
211 by vegetation on the superficial energy exchanges at the level of the walls of prototypes. The
212 briefly presented TRNSYS code makes it possible to establish annual simulations at the real
213 scale of a building. The link between the two programs then allows the estimation of the annual
214 energy needs of a building in the presence of green walls. This involves modifying the initial
215 link between the meteorological data file "Type 99 or Type 15" and the multi-zone building
216 code "Type 56". It is necessary to create a new component, which models the links between the
217 weather file and the green walls. In other words, the new component must provide continuity

235 as vegetated is connected to "Type 155". It will be added to the other boundary conditions from
236 the weather file, and then the program solves the equations [48]. The results are used as an
237 entrance to the green wall of the "Type 56". In other words, for the operation of the program,
238 at each time step (t_0) the green wall model recovers the surface heat flux (provided by the "Type
239 56") in the previous time step (t_{0-1}), solves the GW equations, then returns the determined
240 temperature to "Type 56". The program will then take care of carrying out the energy balances
241 of the building.

242 2.3. *Study and analysis of a detached house*

243 As shown previously, few numerical studies have focused on the evaluation of the thermal
244 interest of green walls on buildings. To this end, the new component developed on TRNSYS
245 was used to bring a new contribution to the prediction of the thermal behavior of green walls.
246 These are simulations carried out on a typical brick masonry house located in Lille, France.
247 These houses were built in the years 1960-70. Studies have already been carried out on this type
248 of construction. [54, 55]. This type of house has low insulation and in some cases no insulation.
249 For our case study, the house consists of two floors (ground floor + one floor) with a total area
250 of 100 m². The one floor is only added to limit the influence of the roof on the energy balance
251 of the ground floor (Fig. 3). Its outer envelope is constructed in solid red bricks (6 * 12 * 24
252 cm) (transmission coefficient $U = 2.273 \text{ W/m}^2/\text{K}$). The study focuses on the analysis of the
253 concealment of the green walls, they were placed on the South and West side of the house. They
254 are considered without vegetation when it comes to simulations on the reference house. In terms
255 of insulation, it has been assumed that the South and West walls do not have any additional
256 insulation. While the North and East walls have an interior insulation layer of 10 cm ($U_{\text{global}} =$
257 $0.335 \text{ W/m}^2/\text{K}$). It was considered that the percentage of glazing is 20% on each of the facades.
258 As for the internal thermal gains, they were assumed to be zero and the air infiltration was set
259 at 0.6 vol/h. The influence of the vegetation on the microclimatic scale was not addressed in

260 this study, the numerical study case is considered without any joint ownership in the
261 surroundings. In addition, the simulations presented relate only to the ground floor (DRC).



262

263

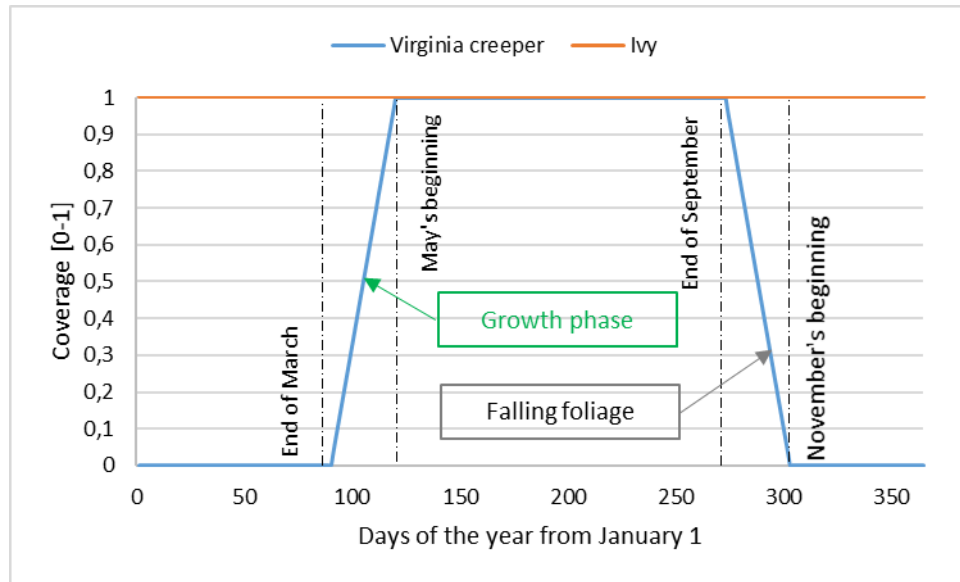
Fig. 3 : Numerical case study

264 Given the absence of historical meteorological data specific to the city of Lille in TRNSYS, a
265 standard file in "user" format was used (TYPE 99). It was created on the basis of data recorded
266 by the weather station between September 01, 2014 and August 31, 2015.

267 2.4. *Definition of scenarios*

268 The hypotheses of the scenarios are based on the French Energy code with articles R.241-25 to
269 R.241-29 [56]. It establishes the obligation to limit the heating temperature in buildings. For
270 example, article R.241-26 specifies that in premises for residential use, the upper heating
271 temperature limits are set on average at 19°C. For all the simulations, the set temperature in
272 winter (heating period: October to April) is set at 19°C during the day and at 15°C at night.
273 While the set temperature for air conditioning is set at 25°C (May to September). Likewise,
274 blackout curtains are supposed to be drawn on the windows when the incident solar radiation
275 exceeds 600 W/m² (only during summer to limit overheating by the glazing). Regarding the
276 type of vegetation, the west and south walls are considered, covered either by ivy or by Virginia

277 creeper during simulations on the green house. The leaf area index (F) considered for the two
 278 plants is 4, while their average thicknesses are set at 12 cm. As for the coverage rate (σ_{gw}), it is
 279 100% for ivy (persistent plant) throughout the year. Depending on the season, this fluctuates
 280 between 0 and 100% for Virginia creeper (deciduous plant) (Fig. 4).



281

282

Figure 4 : Plant growth cycle (model assumption)

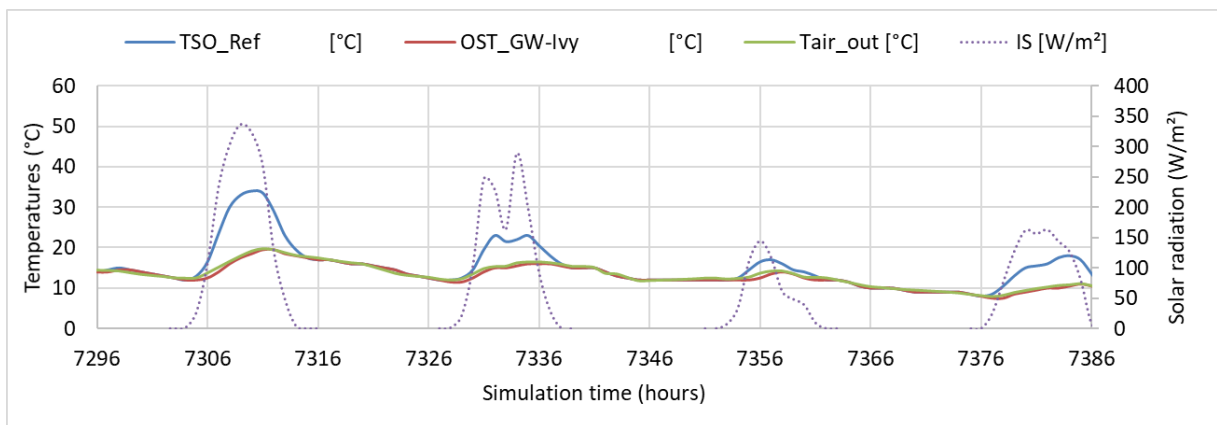
283 For both types of plants as well, GWs are considered directly related to facades (without the
 284 intermediary of an air gap).

285 III. Results and discussion

286 The first simulations were carried out on the green house (ivy) and the reference house in order
 287 to verify the influence of permanent vegetation. The results are presented through comparisons
 288 between variations in Outside Surface Temperature (TSO) and Interior Surface Temperature
 289 (TSI) of southern walls and Operating Temperatures (TOP) in winter and summer and incident
 290 solar radiation (IS). The winter period was studied with two cases of sunshine (weak and strong)
 291 Then, some analyzes are approached on the variation of the energy needs in terms of heating
 292 and air conditioning, in the cases of the presence of GW of the persistent type (ivy) and GWs
 293 of the deciduous type (Virginia creeper).

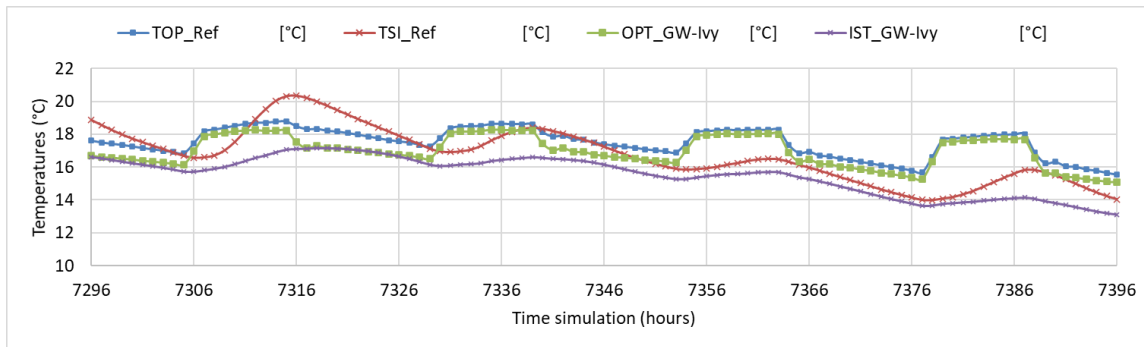
294 3.1. Winter period

295 During periods of winter with little sunlight, the exterior surface (south wall) temperatures of
296 the green house were nearly identical to the ambient air temperatures. They varied between
297 7.5°C and 19.5°C. While the exterior surface temperatures of the reference house (south wall)
298 fluctuated between 8 °C and 34 °C. The difference between the two temperatures corresponding
299 to a minimum peak of incident solar radiation (144 W/m² at 7356 hours) during this sequence
300 was 4°C. This difference is even more amplified with levels of sunshine approaching 200 W/m².
301 It reached 14.5°C as a maximum value during a peak of incident solar radiation of 336 W/m²
302 (Fig. 5).



303
304 **Fig. 5 : Comparison between the temperatures of the exterior surfaces of the southern walls**
305 **of the two houses (winter sequence with weak sunshine)**

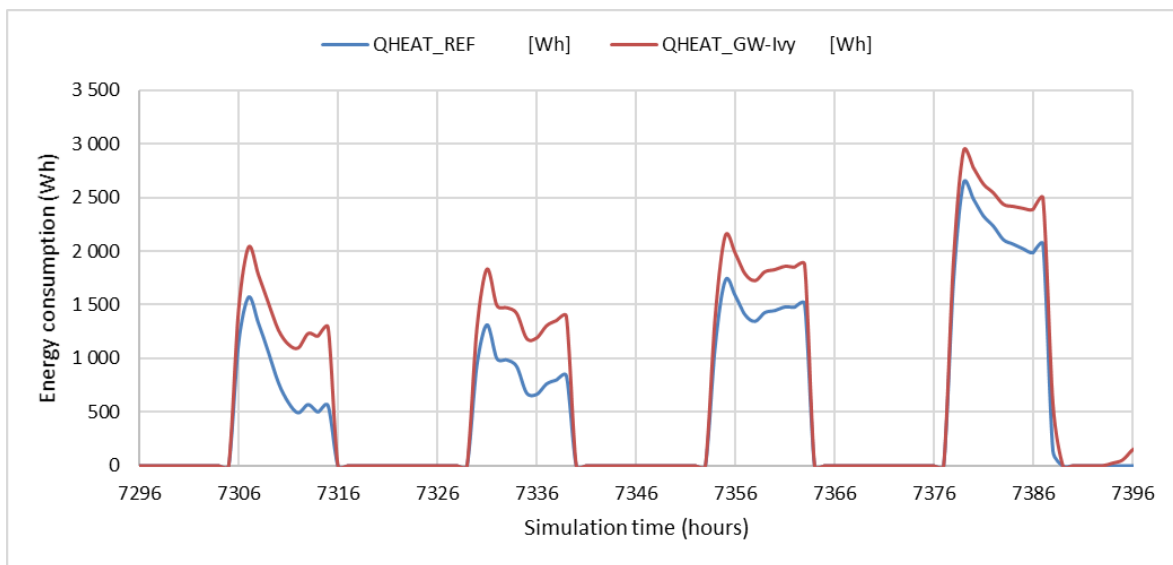
306 As for the interior surface temperatures, they were between 14°C and 20°C for the south wall
307 of the reference house. At the level of the vegetated house, these varied between 13.6°C and
308 17.2°C. Because of these low interior surface temperatures, operating temperatures were greatly
309 influenced by heating. They practically closely followed the setpoint temperature variations in
310 the case of the green house and were slightly higher for the reference house (Fig. 6).



311

312 ***Fig. 6 : Comparison between the interior surface temperatures and the operative***
 313 ***temperatures of the two houses (winter sequence with low sunshine)***

314 These slight differences in terms of operating temperatures, caused mainly by the differences
 315 in temperature of the exterior and interior surfaces, resulted in a greater energy demand in the
 316 case of the presence of plants. Indeed, the presence of vegetation on the south and west walls
 317 has slightly limited the solar energy contributions on these facades. This led to heating energy
 318 requirements on average 180 Wh higher in the green house than those of the reference house
 319 (Fig. 7).

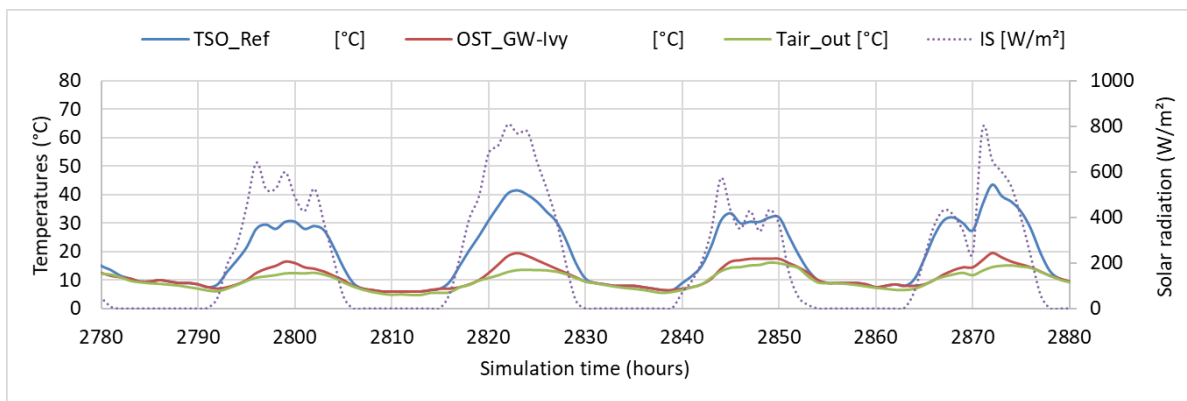


320

321 ***Fig. 7 : The variation in the energy demand for heating in the two houses (winter sequence***
 322 ***with little sunshine)***

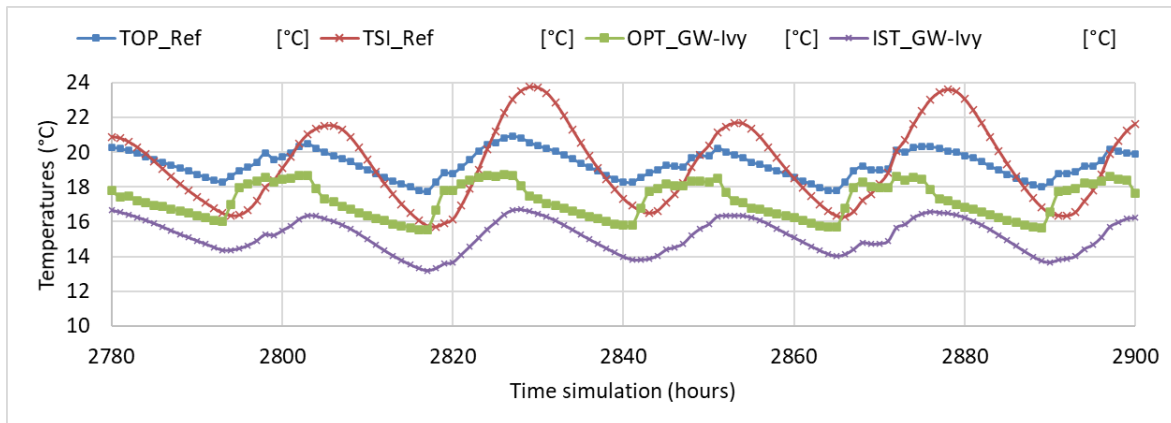
323 Figure 8 illustrates the temperature fluctuations of the exterior surfaces of the south walls of the
 324 two houses (with or without GW) during the winter period. This second sequence of the winter

325 period is characterized by very high levels of sunshine compared to the average incident solar
 326 radiation usually recorded in Lille. Indeed, the incident solar radiation peaks oscillated between
 327 574 W/m² and 809 Wm². The differences between the surface temperatures of the vegetated
 328 wall and those of the reference wall corresponding to these two solar radiation peaks were
 329 14.5°C and 22°C respectively. During this winter sequence with very high levels of sunshine,
 330 the reference wall gained 22°C on average compared to the ambient air temperatures. However,
 331 the surface temperature gains of the vegetated wall were limited by only 4°C on average.



332
 333 **Fig. 8 : Comparison between the temperatures of the exterior surfaces of the south walls of**
 334 **the two houses (winter sequence with sunshine)**

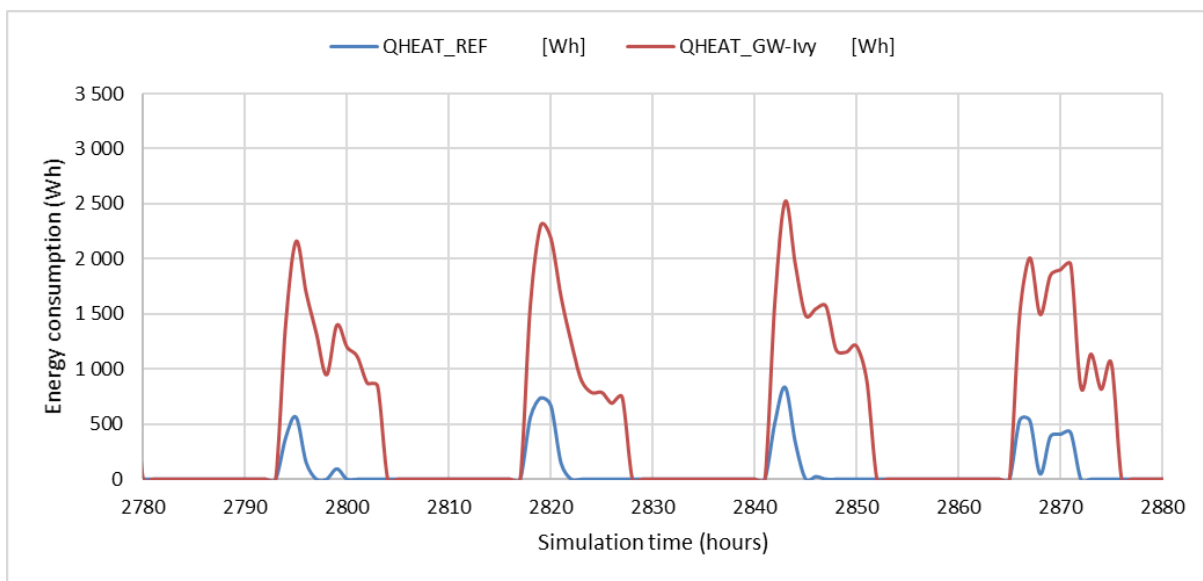
335 These large differences between the surface temperatures of the south wall of the reference
 336 house and that of the green house had direct repercussions on variations in interior surface
 337 temperatures and operating temperatures. Indeed, the (TSI_Ref) had values between 15.7°C
 338 and 23.8°C. These values significantly increased the operating temperatures. This allowed the
 339 reference house to limit the use of heating. With regard to the green house, the limitation of
 340 solar energy inputs has resulted in interior surface temperatures well below the set point
 341 temperatures. They were between 13.2°C and 16.7°C. As a result, the operating temperatures
 342 were more influenced by the heating, and nearly matched the set point temperatures (Fig. 9).



343

344 ***Fig. 9 : Comparison between the interior surface temperatures and the operating***
 345 ***temperatures of the two houses (winter sequence with sunshine)***

346 Figure 10 illustrates the impact of limiting solar energy gains on the energy demand of the two
 347 houses. During the very sunny winter period, the presence of green walls on the west and south
 348 facades had a negative influence on the energy needs for heating. These were on average 478
 349 Wh higher in the green house than those in the reference house.



350

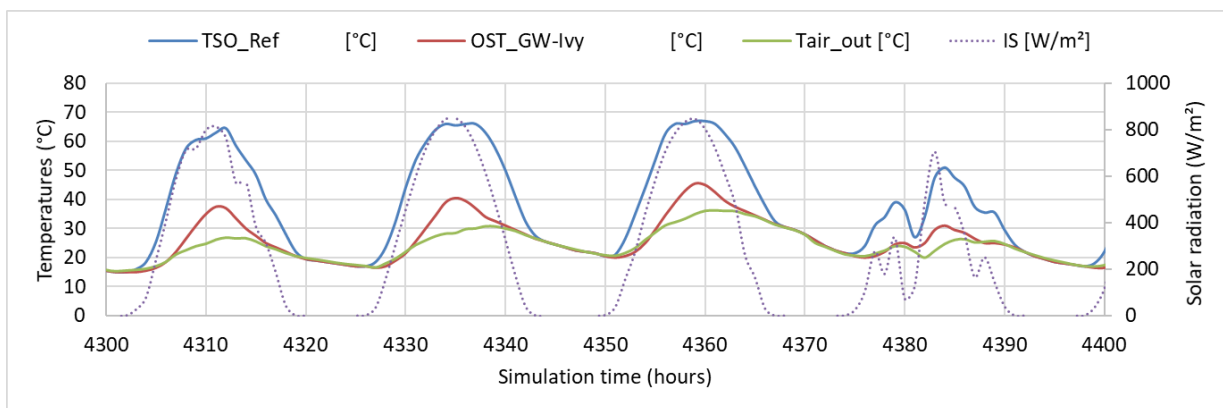
351 ***Fig. 10 : The variation in energy demand for heating in the two houses (winter sequence***
 352 ***with sunshine)***

353 It is important to emphasize that the presence of plants under other winter weather conditions
 354 (very cold day, strong gusts of wind, etc.) could provide buildings with positive effects in terms
 355 of limiting energy needs [57-59]. However, for a better optimization of the benefits which could

356 be brought by the plants, the results obtained led us to recommend the use of deciduous plants
 357 (which lose their foliage in winter) on the South and West facades so as not to limit the solar
 358 energy gains in winter. Evergreen plants, on the other hand, can be used on facades that receive
 359 less solar radiation during winter (North and East).

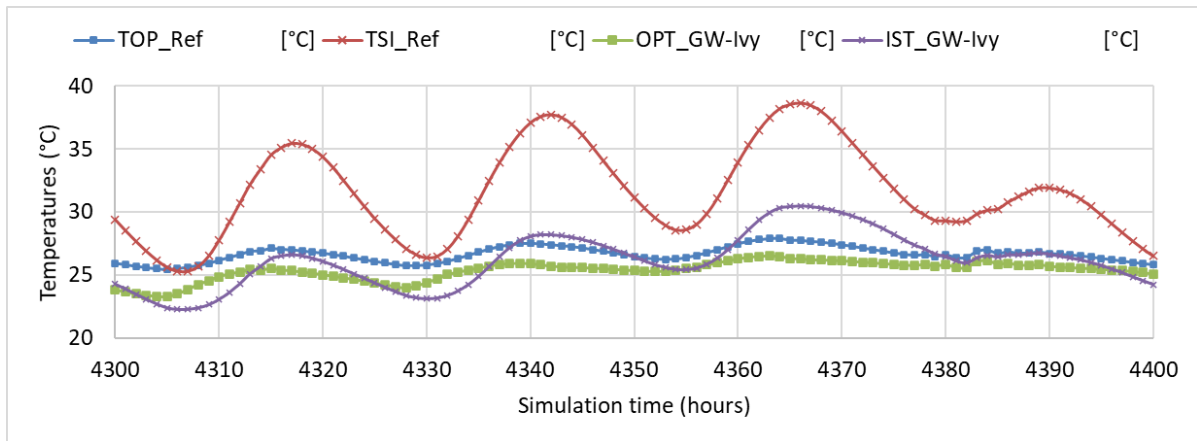
360 3.2. Summer period

361 In summer, the comparison between the temperatures of the exterior surfaces of the green house
 362 and those of the reference house shows spectacular results. For the sequence chosen, the surface
 363 temperatures of the south wall of the ordinary house reached 65°C and 67°C during the solar
 364 radiation photos (813 to 850 W/m²). While those of the green house did not exceed 37°C and
 365 45°C under solar radiations of 813 W / m² and 850 W/m² respectively (Fig. 11).



366
 367 **Fig. 11 : Comparison between the temperatures of the exterior surfaces of the south walls**
 368 **of the two houses (summer sequence)**

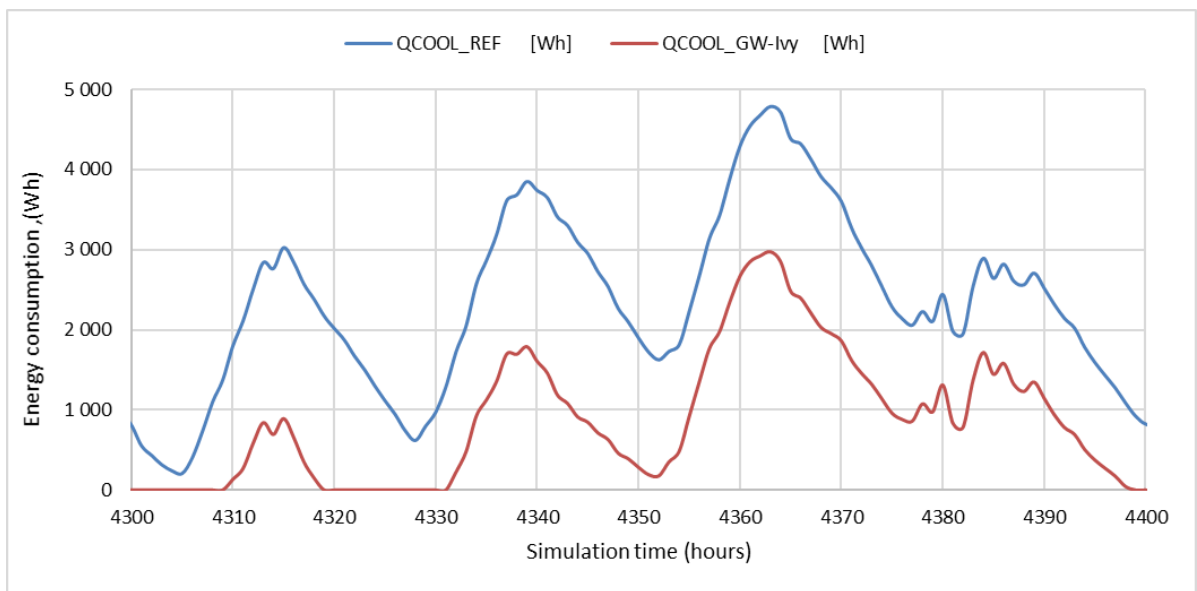
369 Inside both houses, the interior surface temperatures of the regular house were much higher
 370 than those of the green house. They reached 38°C as the maximum value while those of the
 371 green house were limited to 30.5°C. Beyond reducing energy needs, reducing interior surface
 372 temperatures contributes to improving thermal comfort for users. Indeed, the results obtained
 373 showed that the operating temperatures were 1.3°C higher on average in the reference house
 374 than those of the green house (Fig. 12).



375

376 **Figure 12 : Comparison between the interior surface temperatures and the operating**
 377 **temperatures of the two houses (summer sequence)**

378 The differences in terms of interior surface temperatures, caused by the limitation of summer
 379 overheating by plants, resulted in a higher energy demand for air conditioning in ordinary
 380 houses than in green houses. The reduction in energy requirements was proportional to the
 381 reduction in surface temperatures. These were 1463 Wh higher on average in the reference
 382 house than the green house (Fig. 13).



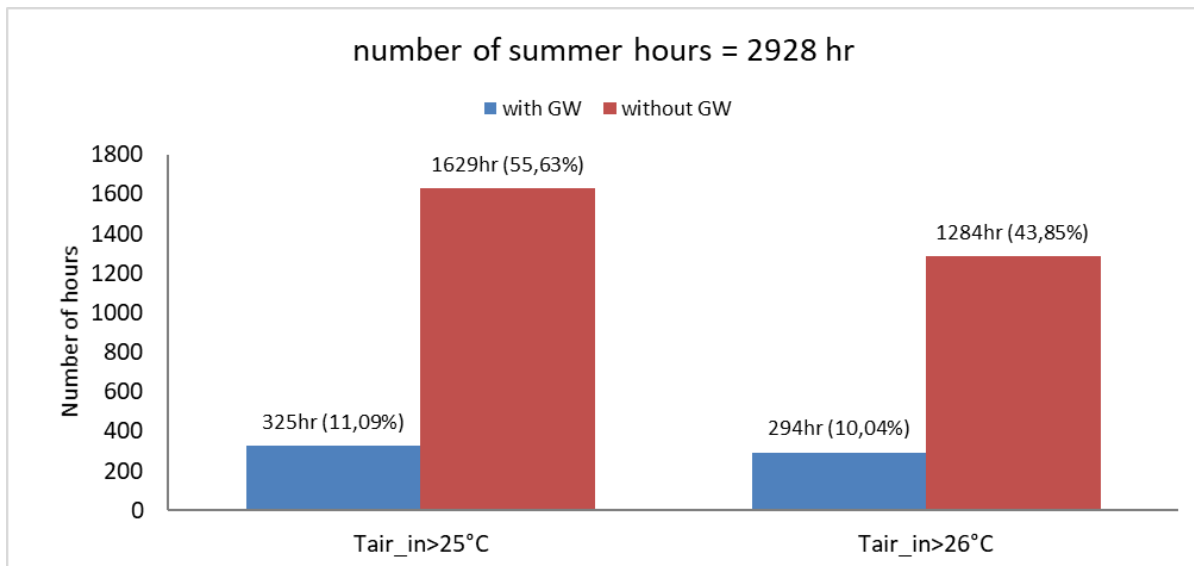
383

384 **Fig. 13 : The variation in energy demand for air conditioning in the two houses**

385 Furthermore, since air conditioning is not commonly used in single-family homes in Lille, other
 386 simulations were carried out to illustrate the influence of vegetation on improving indoor

387 thermal comfort in summer. These are the same criteria used for the simulations presented
388 above with the deactivation of the air conditioning.

389 Figure 14 compares the number of hours during which the indoor air temperatures of the two
390 houses were either 25°C or 26°C higher. It shows that the air temperature in the ordinary house
391 exceeds 25°C for 1,629 hours, or 55.63% of the total number of hours in the summer period.
392 Unlike the green house, the number of hours during which the air temperature exceeded 25°C
393 was limited to 325 hours, representing only 11.09% of the total number of hours during the
394 summer period.



395

Fig. 14 : Number of hours in a situation of thermal discomfort

396

397 By taking 26°C as a comfort threshold, the number of hours during which the ordinary house
398 is estimated in a situation of discomfort is 990 hours higher than in the green house, i.e. a total
399 of 1284 hours during which the temperature air inside the ordinary house has exceeded 26°C.

400 This represents 43.85% of the total number of hours in the summer period, unlike the green
401 house where the percentage of time spent in a situation of thermal discomfort was only 10.04%
402 (294 hours).

403

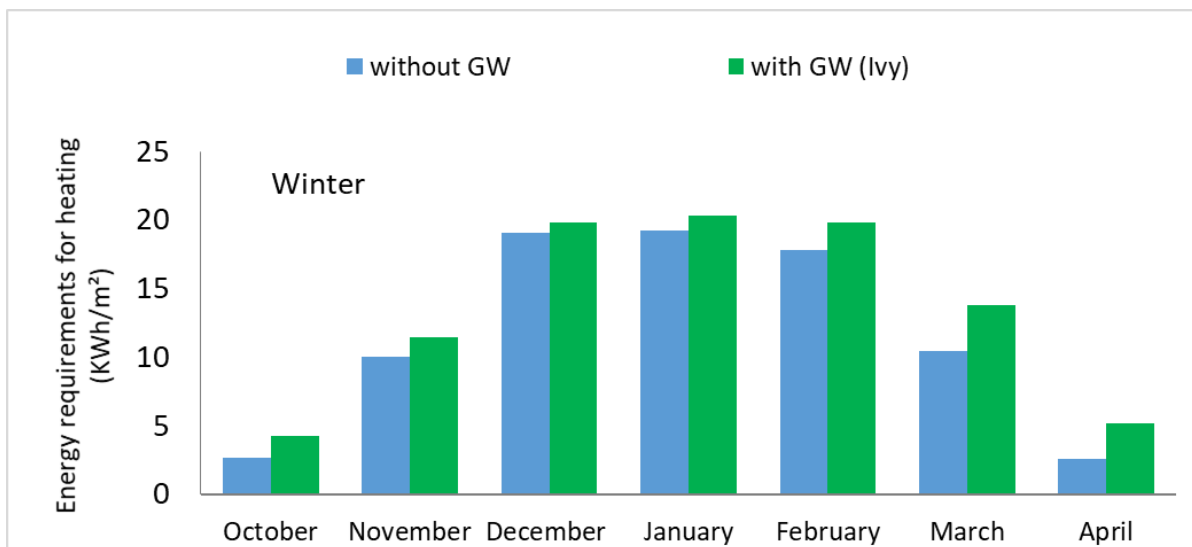
404

405 3.3. *Influence of vegetation on annual energy demand*

406 In order to assess the impact of green walls on the annual energy demand of the house studied,
407 the results of simulations of energy demands for heating and air conditioning for each type of
408 vegetation (ivy or Virginia creeper) are compared with those of the reference house.

409 3.3.1. *Influence on energy demand during winter*

410 In the case of using ivy (evergreen plant), the energy demand for heating was greater than that
411 of the ordinary house. Indeed, as was explained during the comparisons of surface temperatures,
412 the presence of plants prevented the facades from benefiting from solar energy inputs. These
413 were found with interior surface temperatures well below the defined comfort threshold (15°C
414 at night and 19°C during the day). This induces the use of greater heating power with longer
415 periods than in the ordinary house (Fig. 15).

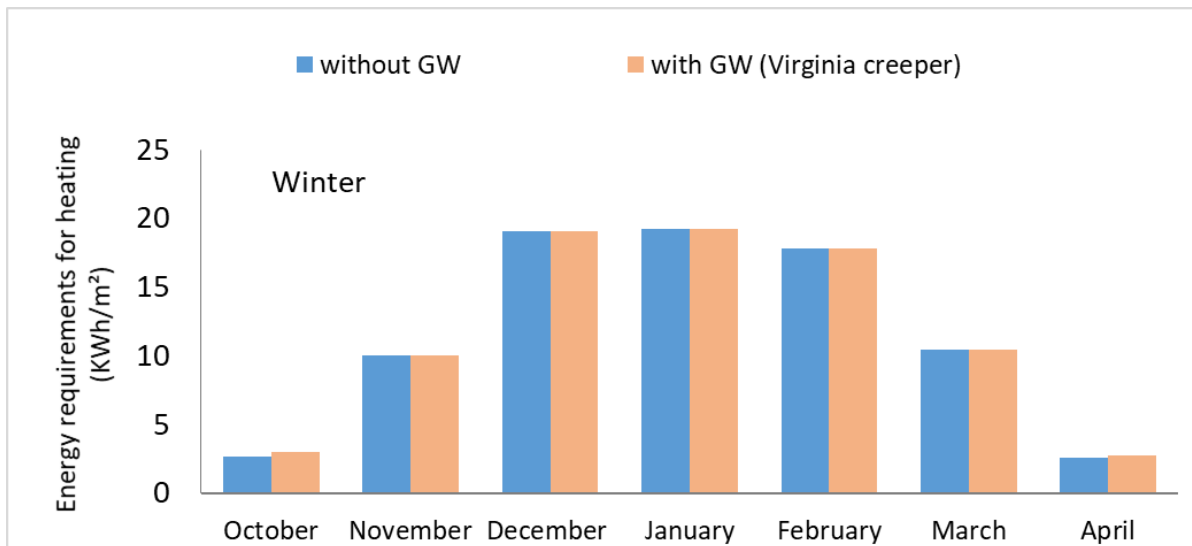


416

417 ***Fig. 15 : Comparison of the heating needs between an ordinary house and a house with***
418 ***green walls (Ivy)***

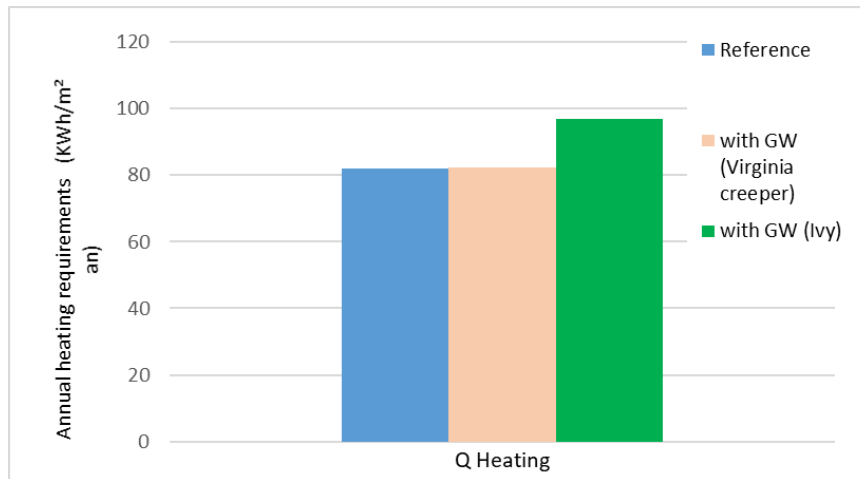
419 The differences were more accentuated during the months of March and April which were
420 particularly marked by sunny days. The green house consumed during these two months
421 approximately 3 kWh/m² in heating more than the ordinary house. During the rest of the winter

422 period, the energy demand for heating of the ordinary house was lower by 1.37 kWh/m² on
 423 average than that of the house equipped with GW with evergreen leaves (ivy).
 424 The house equipped with Virginia creeper thanks to the loss of foliage during winter allowed
 425 the facades to benefit from solar energy input, the energy consumption in terms of heating was
 426 similar to that of the ordinary house. It reached a maximum of 19.24 kWh/m² during the coldest
 427 month (January) and 10.22 kWh/m² on average during the months of March and November. In
 428 addition, slight deviations were noted during the beginning of the growth phases of the plants
 429 and the fall of the foliage. They are of the order of 0.31, and 0.13 kWh/m² for the months of
 430 October and April respectively (Fig. 16).



431
 432 **Fig. 16 : Comparison of the heating needs between an ordinary house and a house with**
 433 **green walls (Virginia creeper)**

434 In terms of annual energy consumption, the simulations showed that the heating requirements
 435 for the ordinary house were 81.86 kWh/m²/year. The presence of ivy has increased these by
 436 18.14%, or an annual consumption of 96.87 kWh.m⁻²/year. Unlike the Virginia creeper which
 437 amplified the energy demand for heating by only 0.45 kWh/m²/year, i.e. an excess consumption
 438 of only 0.54% compared to the reference house (Fig. 17).



439

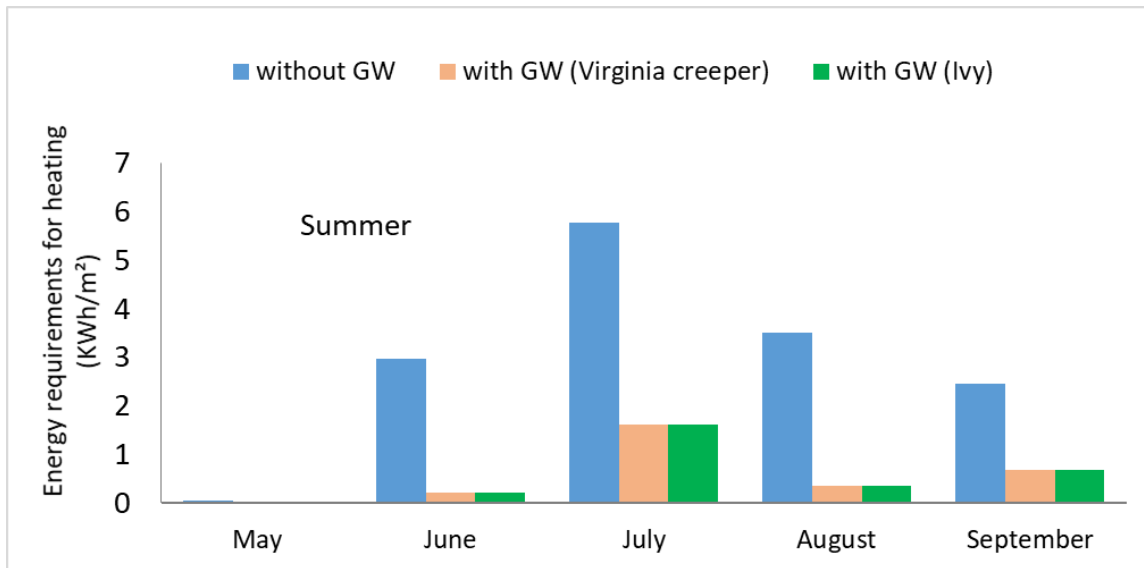
440

Fig. 17 : Annual report on energy needs for heating

441 The choice of the type of plants is therefore of great importance, it must be made according to
 442 the climatic conditions of the region. Thus, the use of GW with evergreen leaves is strongly
 443 discouraged on facades that capture more solar radiation because of their negative influence on
 444 the energy balance in winter.

445 *3.3.2. Influence on energy demand in summer*

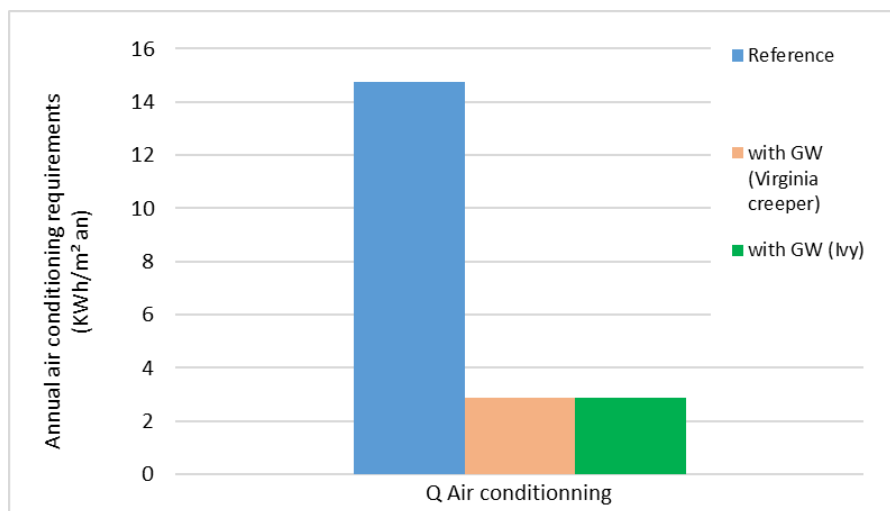
446 In summer, the presence of green walls significantly reduced the air conditioning load. Virginia
 447 creeper and ivy reduced energy demand for air conditioning by 4.16 kWh/m² for the hottest
 448 month (July). During the months of June, August and September the reduction in air
 449 conditioning load was 2.76, 3.15 and 1.76 kWh/m² respectively by GW compared to the
 450 ordinary house (Fig. 18).



451

452 **Fig. 18 : Comparison of air conditioning needs between an ordinary house and a house**
 453 **with green walls (Ivy and Virginia creeper)**

454 The reduction in the air conditioning load is linked to the cooling provided by the plants, which
 455 by their presence reduce the heat flow received by the green facades. The reduction in summer
 456 overheating by the presence of vegetation was estimated at 11.89 kWh/m²/year, ie a decrease
 457 of 80.56% relative to the reference house (Fig. 19).



458

459 **Fig. 19 : Annual review of air conditioning energy needs**

460 In terms of quantitative results related to energy consumption, it is important to emphasize that
 461 the latter are very sensitive to the performance of the devices used (air conditioning or heating)

462 and to the set point temperatures. Note also that depending on the insulation of the walls, the
 463 degree of influence of the vegetation is very different (paragraph 3.4).

464 *3.4. Influence of GW a function of the thermal resistance of the building envelope*

465 Other simulations were carried out with the objective of evaluating the impact of GWs based
 466 on the thermal resistance of the facades. The thermal resistance of the south and west walls of
 467 the green house was gradually increased by increasing the thickness of the added insulation
 468 layer (Table 1).

469 The GW with ivy placed on the south facade made it possible to reduce the average and
 470 maximum interior surface temperature by 2.85°C and 8.16°C in the case of the uninsulated
 471 wall. However, these reductions were limited to 0.23°C (average TSI) and 0.35°C (maximum
 472 TSI) in the case of 30 cm insulation. In terms of air conditioning load, the table shows a
 473 reduction of only 13.85% for an insulation of 30cm. Unlike the uninsulated configuration where
 474 the reduction in energy needs for air conditioning was estimated at 80.56% relative to the
 475 ordinary house.

476 **Table 1 : Influence of vegetation depending on the level of insulation of the wall**

| Insulation (cm) | Average TSI | | Maximum TSI | | Minimum TSI | | Heating requirements (kWh/m ² /year) | | Air conditioning requirements (kWh/m ² /year) | | Total requirements (kWh/m ² /year) | |
|--------------------|-------------|-------|-------------|-------|-------------|-------|--|-------|---|-------|--|-------|
| | Ref | GW | Ref | GW | Ref | GW | Ref | GW | Ref | GW | Ref | GW |
| | 0 | 18.86 | 16.01 | 38.64 | 30.48 | 8.29 | 8.12 | 82.00 | 96.87 | 14.76 | 2.87 | 96.76 |
| 5 | 19.82 | 18.84 | 29.20 | 27.53 | 13.52 | 13.34 | 56.94 | 60.55 | 8.95 | 4.74 | 65.89 | 65.28 |
| 10 | 19.99 | 19.39 | 28.50 | 27.51 | 14.28 | 14.17 | 52.96 | 54.99 | 8.18 | 5.56 | 61.14 | 60.54 |
| 15 | 20.05 | 19.62 | 28.22 | 27.54 | 14.59 | 14.51 | 51.34 | 52.75 | 7.86 | 5.97 | 59.20 | 58.72 |
| 20 | 20.09 | 19.76 | 28.07 | 27.55 | 14.76 | 14.70 | 50.46 | 51.54 | 7.69 | 6.21 | 58.15 | 57.75 |
| 25 | 20.11 | 19.84 | 27.98 | 27.56 | 14.87 | 14.81 | 49.90 | 50.78 | 7.59 | 6.36 | 57.49 | 57.14 |
| 30 | 20.13 | 19.90 | 27.92 | 27.57 | 14.94 | 14.89 | 49.52 | 50.26 | 7.51 | 6.47 | 57.03 | 56.73 |

477

478 Below an insulation thickness of 5 cm, the influence of plants in reducing air conditioning needs
479 becomes less important, it goes from 11.89 kWh/m²/year (0 cm of insulation) to 4.21
480 kWh/m²/year (5 cm of insulation) to decrease further progressively to 1.04 kWh/m²/year for an
481 insulation of 30 cm.

482 These results confirm the positive role that vegetation can make, if they are used on old houses
483 with little insulation. Other studies done on ivy [60] (*Boston Ivy*) or different evergreen-type
484 plants (*Pandorea jasminoides* variegated and *Rhyncospernum jasminoides*) [61] or on deciduous
485 Chinese wisteria [62] show methodologies and results similar to ours on the interest of green
486 walls. Thus, vegetation can contribute significantly for the thermal renovation of old buildings.
487 In the case of new constructions, the use of GWs cannot be considered for the thermal criterion
488 alone. Finally, although GWs are not suitable for new constructions from a thermal point of
489 view, the use of this technique could be recommended based on the other advantages of
490 vegetation (urban heat island, air pollution control, biodiversity, aesthetics, etc.).

491 **IV. Conclusions**

492 The integration of a model developed in a TRNSYS environment made it possible to assess the
493 thermal impact of the use of Green Walls on buildings. The main conclusions are:

- 494 1. The simulations show that it is not necessary to have a great thickness of green walls to
495 obtain good performance, the ideal is to be between 5 and 20cm. The GW on the south
496 facade made it possible to reduce overheating in rooms in the South.
- 497 2. the evaluation of the thermal impact of the use of GWs on buildings. The various
498 simulations carried out on the brick house highlighted the thermal advantages that GWs
499 can provide during the summer. Indeed, the comparisons between the variations in the
500 surface temperatures of the green house and the ordinary one has shown great
501 differences. These reached up to 37.5°C as a maximum value during the summer. Thus,
502 the presence of vegetation protected the facades against summer overheating. This

503 consequently reduced the energy requirements for air conditioning which were 80.56%
504 lower than those of the non-vegetated house.

505 3. the impact of the presence of plants on heating consumption in winter was negative. The
506 increase in energy needs for heating was very important during sunny days because of
507 the limitation of solar energy inputs by plants. We must therefore recommend the use
508 of deciduous plants on facades exposed to the sun so that they take advantage of solar
509 radiation (in winter) and limit energy demand for heating. The simulations carried out
510 on the green house with deciduous plants showed that the energy demand in winter was
511 similar to the non-green house and the energy gains in the summer period were very
512 important.

513 4. the study of the influence of vegetation as a function of the thermal resistance of the
514 facades. It made it possible to underline that the GWs technique is more suitable for the
515 thermal renovation of uninsulated or poorly insulated buildings than well-insulated new
516 constructions.

517 5. It is therefore possible for design offices to integrate the performance of green walls in
518 the calculations of energy balances. This work also makes it possible to promote SMI-
519 SMEs (small and medium-sized industries/enterprises) in the implementation of green
520 walls.

521

522 **Acknowledgement**

523 This research was conducted out at the Laboratory of Civil Engineering and Geo-Environment
524 of University of Artois, the Graduate School of Engineering HEI of Lille in the context of the
525 project “Building and Positive Biodiversity” (2012-2015), supported by the Catholic University
526 of Lille, the “Nord-Pas-de-Calais” Regional Council and the European Metropolis of Lille.

527

528 **Bibliography:**

- 529 [1] M. Köhler, Green facades—a view back and some visions, *Urban Ecosyst.* 11(2008) 423–
530 436, <http://dx.doi.org/10.1007/s11252-008-0063-x>.
- 531 [2] T. Susca, S.R. Gaffin, G.R. Dell’Osso, Positive effects of vegetation: Urban heat island and
532 green roofs, *Environ. Pollut.* 159 (2011) 2119–2126. <https://doi:10.1016/j.envpol.2011.03.007>.
- 533 [3] E.J. Gago, J. Roldan, R. Pacheco-Torres, J. Ordóñez, The city and urban heat islands: A
534 review of strategies to mitigate adverse effects, *Renew. Sust. Energ. Rev.* 25 (2013) 749–758.
535 <https://doi:10.1016/j.rser.2013.05.057>
- 536 [4] R. Djedjig, R. Belarbi, E. Bozonnet, Experimental study of green walls impacts on buildings
537 in summer and winter under an oceanic climate, *Energy Build.* 150 (2017) 403–411.
538 <https://doi:10.1016/j.enbuild.2017.06.032>.
- 539 [5] U. Mazzali, F. Peron, P. Romagnoni, R.M. Pulselli, S. Bastianoni, Experimental
540 investigation on the energy performance of Living Walls in a temperate climate. *Build. Environ.*
541 64 (2013) 57–66, <http://dx.doi.org/10.1016/j.buildenv.2013.03.005>.
- 542 [6] M. Haggag, A. Hassan, S. Elmasry, Experimental study on reduced heat gain through green
543 facades in a high heat load climate. *Energy Build.* 82 (2014) 668–674,
544 <http://dx.doi.org/10.1016/j.enbuild.2014.07.087>.
- 545 [7] K. Perini, M. Ottel , A.L.A. Fraaij, E.M. Haas, R. Raiteri, Vertical greening systems and
546 the effect on air flow and temperature on the building envelope. *Build. Environ.* 46 (2011)
547 2287–2294, <http://dx.doi.org/10.1016/j.buildenv.2011.05.009>.
- 548 [8] M.A. Kenai, L. Libessart, S. Lassue, D. Defer, Impact of plants occultation on energy
549 balance: Experimental study. *Energy Build.* 162 (2018) 208–218.
550 <https://doi.org/10.1016/j.enbuild.2017.12.024>.
- 551 [9] R. Djedjig, M. El Ganaoui, R. Belarbi, R. Bennacer, Thermal effects of an innovation green
552 all on building energy performance, *Mech. Ind.* 18, 104 (2017)

- 553 [10] J. Coma, G. Pérez, A. de Gracia, S. Burés, M. Urrestarazu, L.F. Cabeza, Vertical greenery
554 systems for energy savings in buildings: A comparative study between green walls and green
555 facades. *Build. Environ.* 11 (2017) 228-237
- 556 [11] N.H. Wong, A.Y. Kwang Tan, Y. Chen, K. Sekar, P.Y. Tan, D. Chan, K. Chiang,
557 N.C.Wong, Thermal evaluation of vertical greenery systems for building walls, *Build. Environ.*
558 45 (2010) 663–672, <http://doi.org/10.1016/j.buildenv.2009.08.005>.
- 559 [12] E. Cuce, Thermal regulation impact of green walls: An experimental and numerical
560 investigation, *Appl. Energy.* 194 (2017) 247–254. <http://doi:10.1016/j.apenergy.2016.09.079>.
- 561 [13] F. Convertino, G. Vox, E. Schettini, Heat transfer mechanisms in vertical green systems
562 and energy balance equations. *Int. J. Des. Nat. Ecodyn.*, 1:14 (2019) 7-18.
563 <https://doi.org/10.2495/DNE-V14-N1-7-18>
- 564 [14] L.L.H .Peng, Z. ,Jiang, X.Yang, Q. Wang, Y. He, S. S. Chen, Energy savings of block-
565 scale facade greening for different urban forms, *Appl. Energy.* 279 (2020) 115844
566 <https://doi.org/10.1016/j.apenergy.2020.115844>.
- 567 [15] I. Oberti, F. Plantamura, The inclusion of natural elements in building design: the role of
568 green rating systems. *Int. J. Sustain. Dev. Plan.*, 2:12 (2017) 217-226
569 <https://doi.org/10.2495/SDP-V12-N2-217-226>
- 570 [16] J. Li, B.Zheng, X. Chen, Z. Qi, K. B.Bedra, J. Zheng, Z. Li, L. Liu, Study on a full-year
571 improvement of indoor thermal comfort by different vertical greening patterns. *J. Build. Eng.*
572 35 (2021) 101969 <https://doi.org/10.1016/j.job.2020.101969>.
- 573 [17] Z. Azkorra, G. Pérez, J. Coma, L.F. Cabeza, S. Bures, J.E. Álvaro, A. Erkoreka, M.
574 Urrestarazu, Evaluation of green walls as a passive acoustic insulation system for buildings,
575 *Appl. Acoust.* 89 (2015) 46–56. <https://doi:10.1016/j.apacoust.2014.09.010>.

- 576 [18] T. Van Renterghem, D. Botteldooren, Reducing the acoustical façade load from road
577 traffic with green roofs, *Build. Environ.* 44 (2009) 1081–1087.
578 <https://doi:10.1016/j.buildenv.2008.07.013>.
- 579 [19] N.H. Wong, A.Y. Kwang Tan, P.Y. Tan, K. Chiang, N.C. Wong, Acoustics evaluation
580 of vertical greenery systems for building walls, *Build. Environ.* 45 (2010) 411–420.
581 <https://doi:10.1016/j.buildenv.2009.06.017>.
- 582 [20] T. Eniolu Morakinyoa, A. Lai, K. Ka-Lun Lau, E. Ng. Thermal benefits of vertical
583 greening in a high-density city: Case study of Hong Kong, *Urban. For. Urban. Green.* 37 (2019)
584 42–55
- 585 [21] C.Y. Jim, Assessing growth performance and deficiency of climber species on tropical
586 greenwalls, *Landsc. Urban. Plan.* 137 (2015) 107–121
- 587 [22] Y. He, H. Yu, A. Ozaki, N. Dong, S. Zheng, An investigation on the thermal and energy
588 performance of living wall system in Shanghai area, *Energy Build.* 140 (2017) 324–335.
589 <http://doi:10.1016/j.enbuild.2016.12.083>.
- 590 [23] J. Yoshimi, H. Altan, Thermal Simulations on the effects of vegetated walls on indoor
591 building environments, *Proceedings of Building Simulation, 12th Conference of International*
592 *Building Performance Simulation Association, Sydney, 2011*
- 593 [24] T. Koyama, M. Yoshinaga, K. Maeda, A. Yamauchi, Transpiration cooling effect of
594 climber greenwall with an air gap on indoor thermal environment, *Ecol. Eng.* 83 (2015) 343–
595 353
- 596 [25] M. Ottel , H.D. van Bohemen, A.L.A. Fraaij, Quantifying the deposition of particulate
597 matter on climber vegetation on living walls, *Ecol. Eng.* 36 (2010) 154–162.
598 <https://doi:10.1016/j.ecoleng.2009.02.007>.
- 599 [26] R. Djedjig, E. Bozonnet, R. Belarbi, Modelling green wall interactions with street canyons
600 for building energy simulation in urban context, *Urban Clim.* 16 (2016) 75–85

601 [27] L. Malys, M. Musy, C. Inard, Direct and indirect impacts of vegetation on Building
602 confort: A comparative study of lawns, green walls and green roofs. *Energies*. 1:9 (2016) 32.
603 <https://doi.org/10.3390/en9010032>

604 [28] D.C. Kalani, L.C. Cheuk, Comparative reduction of building cooling load through green
605 roofs and green walls by EnergyPlus simulations. *Build. Simul.* 11 (2018) 421- 434

606 [30] M.S. Ahamed, H. Guo, K. Tanino, Modeling heating demands in a Chinese-style solar
607 greenhouse using the transient building energy simulation model TRNSYS, *J. Build. Eng.* 29
608 (2020) 101114

609 [31] S.-E. Ouldboukhitine, R. Belarbi , D. J. Sailor, Experimental and numerical investigation
610 of urban street canyons to evaluate the impact of green roof inside and outside buildings, *Appl.*
611 *Energy*. 114 (2014) 273–282

612 [32] A. Ávila-Hernández, E. Simáa , J. Xamán , I. Hernández-Pérez , E. Téllez-Velázquez ,
613 M.A. Chagolla-Aranda, Test box experiment and simulations of a green-roof: Thermal and
614 energy performance of a residential building standard for Mexico, *Energy Build.* 209 (2020)
615 109709

616 [33] H. T. Rakotondramiarana, T. Fanomezana Ranaivoarisoa, D. Morau, Dynamic Simulation
617 of the Green Roofs Impact on Building Energy Performance, Case Study of Antananarivo,
618 Madagascar, *Buildings*, 5 (2015) 497-520; <http://doi.org/10.3390/buildings5020497>

619 [34] C. Guattari, L. Evangelisti, F. Asdrubali, R. De Lieto Vollaro, Experimental Evaluation
620 and Numerical Simulation of the Thermal Performance of a Green Roof, *Appl. Sci.* 10 (2020)
621 1767. <http://doi.org/10.3390/app10051767>.

622 [35] E. Mehrinejad Khotbehsara, A. Baghaei Daemei, F. Asadi Malekjahan, Simulation study
623 of the eco green roof in order to reduce heat transfer in four different climatic zones, *Results*
624 *Eng.* 2 (2019) 100010

625 [36] P. Ferrantea, M. La Gennusaa, G. Peria, G. Scaccianocea, G. Sorrentino, Comparison
626 between conventional and vegetated roof by means of a dynamic simulation, *Energy Proc.* 78
627 (2015) 2917 – 2922, 6th International Building Physics Conference, IBPC 2015

628 [37] C. Zeng, X. Bai, L. Sun, Y. Zhang, Y. Yuan, Optimal parameters of green roofs in
629 representative cities of four climate zones in China: A simulation study, *Energy Build.* 150
630 (2017) 118-131. <https://doi.org/10.1016/j.enbuild.2017.05.079>.

631 [38] M.A. Kenai, L. Libessart, S. Lassue, D. Defer, Impact of plants obscuration on energy
632 balance: Theoretical and numerical study, *J. Build. Eng.* 29 (2020) 101112
633 <https://doi.org/10.1016/j.jobee.2019.101112>.

634 [39] N. Choab, A. Allouhi, A. El Maakoul, T. Kousksou, S. Saadeddine, A. Jamil, Review on
635 greenhouse microclimate and application: Design parameters, thermal modeling and
636 simulation, climate controlling technologies, *Solar Energy.* 191 (2019) 109-137.
637 <https://doi.org/10.1016/j.solener.2019.08.042>.

638 [40] J. Shen, S. Lassue, L. Zalewski, D. Huang, Numerical study on thermal behavior of
639 classical or composite Trombe solar walls, *Energy Build.* 39 (2007) 962–974.

640 [41] E. Leang, P. Tittlein, L. Zalewski, S. Lassue, Numerical and Experimental Investigations
641 of Composite Solar Walls Integrating Sensible or Latent Heat Thermal Storage, *Applied Sc.*,
642 10 (200) 1854.

643 [42] D. Mazzeo, N. Matera, C. Cornara, G. Olivetti, P. Romagnoni, L. De Santoli, EnergyPlus,
644 IDA ICE and TRNSYS predictive simulation accuracy for building thermal behaviour
645 evaluation by using and experimental campaign in solar test boxes with and without a PCM
646 module, *Energy Build.* 212 (2020) 109812

647 [43] K. Sudhakar, M. S. Jenkins, S. Mangal, S. Shanmuga Priya, Modelling of a solar desiccant
648 cooling system using TRNSYS-MATLAB co-simulator: A review, *J. Build. Eng.* 24 (2019)
649 100749

650 [44] L. Libessart, M.A. Kenai, Measuring thermal conductivity of green-walls components in
651 controlled conditions, *J. Build. Eng.* 19 (2018), 258-265.
652 <https://doi.org/10.1016/j.jobe.2018.05.016>.

653 [45] A. Roques, *Processionary Moths and Climate Change: An Update*, Chapter 2, Springer,
654 2015. ISBN 978-94-017-9340-7

655 [46] Solar Laboratory of energy (USA), *Manuals of TRNSYS*. University of Wisconsin-
656 Madison, USA, 1994

657 [47] J. Seem, 1987. *Modeling of Heat Transfer in Buildings* (Ph. D. thesis). Wisconsin Madison.

658 [48] B. Gebhart, 1971. *Heat Transfer*, 2ed ed. McGraw-Hill, New York.

659 [49] B. Gebhart, Surface Temperature Calculations in Radiant Surroundings of Arbitrary
660 Complexity - for Gray, Diffuse Radiation. *Int. J. Heat. Mass. Transf.* 3 (1961) 341–346.

661 [50] S. Holst, 1993. Heating load of a building model in TRNSYS with different heating
662 systems. Presented at the TRNSYS-User Day 1993, ZAE Bayern, Stuttgart.

663 [51] P. Voit, Th. Lechner, M. Schuler, 1994. Common EC validation procedure for dynamic
664 building simulation programs - application with TRNSYS. Presented at the Conference of
665 international simulation societies, TRANSSOLAR GmbH, Zürich.

666 [52] G. Mitalas, Transfer function method of calculating cooling loads, heat extraction & space
667 temperature, *ASHRAE Journal*. 14 (1972) 54–56.

668 [53] D. Stephenson, G. Mitalas, Calculation of Heat Conduction Transfer Functions for Multi-
669 Layer Slabs. ASHRAE Annual Meeting, Washington, D.C. 1971.

670 [54] E. Sassine, Z. Younsi, Y. Cherif, A. Chauchois, E. Antczak, Experimental determination
671 of thermal properties of brick wall for existing construction in the north of France, *J. Build.*
672 *Eng.* 14 (2017) 15-23. <https://doi.org/10.1016/j.jobe.2017.09.007>.

673 [55] E. Sassine, Z. Younsi, Y. Cherif, E.Antczak, Frequency domain regression method to
674 predict thermal behavior of brick wall of existing buildings, *Appl. Therm. Eng.* 114 (2017) 24-
675 35, 1359-4311. <https://doi.org/10.1016/j.applthermaleng.2016.11.134>.

676 [56] Energy Code, Sub-section 4: Provisions relating to the limitation of the heating temperature
677 (Articles R241-25 to R241-29), 2015

678 [57] R.W.F. Cameron, J. Taylor, M. Emmett, A Hedera green façade – Energy performance
679 and saving under different maritime-temperate, winter weather conditions. *Build. Environ.* 92,
680 (2015) 111–121. <https://doi.org/10.1016/j.buildenv.2015.04.011>.

681 [58] S.W. Peck, C. Callaghan, B. Bass, M.E. Kuhn, Greenbacks from green roofs: forging a
682 new industry in Canada. 1999.

683 [59] K. Perini, M. Ottel , A.L.A. Fraaij, E.M. Haas, R. Raiteri, Vertical greening systems and
684 the effect on air flow and temperature on the building envelope. *Build. Environ.* 46 (2011)
685 2287–2294. <http://doi.org/10.1016/j.buildenv.2011.05.009>.

686 [60] D. Jinxia et al, Research on the Influence of Vertical Green of Envelope Structure on
687 Indoor Thermal Environment——A study of Zhengzhou city, *IOP Conference Series: Earth
688 and Environmental Science*, Volume 608, International Conference on Urban Construction and
689 Management Engineering 16-18 October 2020, Taiyuan, China

690 [61] I. Blanco, E. Schettini, G. Vox, Effects of vertical green technology on building surface
691 temperature. *Int J Des Nat Ecodyn*, 4:13, (2018) 384 – 394

692 [62] V. Lesjak, L. Pajek, M. Kořir, Indirect green façade as an overheating prevention measure.
693 *J. of Croat. Ass. of Civil Eng., GRADEVINAR*, 7:72 (2020) 569-583.
694 <https://doi.org/10.14256/JCE.2797.2019>.

695

696

697